Structural Analysis of Historical Constructions – Jerzy Jasieńko (ed)
© 2012 DWE, Wrocław, Poland, ISSN 0860-2395, ISBN 978-83-7125-216-7

CALIBRATION OF A NUMERICAL MATERIAL BEHAVIOUR MODEL FOR THE SIMULATION OF MULTI-LEAF STONE MASONRY WALLS

Bruno Silva[1], *Athanasios Pappas*[2], *Maria R. Valluzzi*[3], *Francesca da Porto*[4],*Claudio Modena*[5]

ABSTRACT

This paper presents the calibration of a numerical material behaviour of stone masonry based on experimental results of simple compression tests on single- and three-leaf stone masonry panels, in original and injected condition (1:1 and 2:3 scale), carried out at the University of Padova, using a continuous damage model. The stone masonry panels were simulated considering a homogeneous isotropic material capable of taking into account the joint behaviour of stone, mortar and consolidation material and also the interaction between the internal and external leaves.
In simple compression simulations the model was able to represent well the first crack opening, the ultimate load and deformability along the loading direction. In the shear-compression simulations, satisfactory numerical results were obtained in terms of initial elastic stiffness, maximum horizontal loads and also damage progression.The used behaviour model showed limitations on the simulation of the loading and re-loading behaviour in compression and of the energy dissipation and ultimate diplacement capacity in the shear-compression tests.

Keywords: *Stone masonry, Compression, Shear-compression, FEM, Damage model, Calibration*

1. INTRODUCTION

The calibration of a model is an important preliminary phase on the numerical simulation process of a structure. Constitutive models contain parameters that must be quantified based on experimental tests. Although some of these parameters can be determined explicitly through standardized tests, in the case of stone masonry there is a large scatter that requires an extensive database for the estimation of an average acceptable value, even for walls of the same class/typology. Other parameters can be obtained considering the direct adjustment between the numerical and the experimental curves. It is known that the problem of parameter identification is the optimisation of its estimation through a reverse process, where the deviations between the experimental and theoretical values are minimized. Such a process requires experimental results as starting point, and may involve the use of linear or non-linear error treatment methods in the optimization of the estimation.
The experimental campaign that serve as base to this workconcernssingle and three-leaf stone masonry panels in 1:1 and 2:3 scale built according to the traditional constructive technique and tested at the University of Padova. Half of the three-leaf masonry panels were consolidated using injection strengthening technique with natural hydraulic lime grout. Simple-compression tests were carried out on 4 single-leaf panels (F), on 6 three-leaf stone masonry panels in scale 1:1 (B) and on 6 panels in scale 2:3 (D). Cyclic shear-compression tests with different pre-compression levels were performed on 8 panels in scale 1:1 (C) and on 8 in scale 2:3 (E) [1].
The calibration process consisted in doing a fitting of the behaviour model parameters to the experimental results of the simple- and shear-compression tests on the single- and three-leaf stone

[1] Ph.D., University of Padova, silva@dic.unipd.it
[2] Ph.D. student, University of Padova, athanasios.pappas@unipd.it
[3] AssistantProfessor, University of Padova, valluzzi@dic.unipd.it
[4] AssistantProfessor, University of Padova, daporto@dic.unipd.it
[5] Full Professor, University of Padova, modena@dic.unipd.it

masonry panels. The first calibration of the model was done based on the results of the simple-compression tests, which were later applied on the simulation of the shear-compression tests and recalibrated accordingly. The parameters, required by the used numerical model, that were not obtained experimentally were taken from the bibliography. The simulations were done using a continuum damage model, [2], implemented in the finite element software Cast3M [3].

2. DAMAGE MODEL

The adopted material behaviour model is a continuum damage model based on the Continuum Damage Mechanics, capable of reproducing the material tension / deformation curves, including hardening and softening effects and the mechanisms for recovery of stiffness.The constitutive model incorporates two damage variables (eq. 1), one for tension and another for compression and a plastic deformation tensor for the characterization of the non-linear degradation mechanisms under tensile and compression conditions [4].

$$0 \leq (d^+, d^-) \leq 1 \tag{1}$$

where: d^+= the damage variable in tension, d^-= the damage variable in compression
The damage variables can assume values between 0 and 1, where 0 corresponds to the elastic state and 1 to the collapse state. A basic entity of the model is the "effective stress tensor" which is split into tensile and compressive components in order to clearly distinguish the respective stress contributions (eq. 2).

$$\bar{\sigma} = (1 - d^+)\bar{\sigma}^+ + (1 - d^-)\bar{\sigma}^- \tag{2}$$

where: $\bar{\sigma}$ = the effective stress tensor, $\bar{\sigma}^+$= the tensile stress component, $\bar{\sigma}^-$= the compressive stress component
In the need to define, with precision, if the element is in "load", "unload" or "reload" phase, (Fig. 1), the modelintroduces the concept of equivalent tension associated to a positive scalar value, which is the result of the norm of tensors of effective tensions. The different three-dimensional states of tension can then be compared through a 1D analysis. Following the tensor decomposition adopted by this model, the equivalent tensile and compressive tensions are then considered, being associated to different damage criteria. To apply this numerical model on the simulation of a stone masonry structure it is assumed that initially, i.e., before the application of any load or load cycle, the material is isotropic and homogeneous.
For this study it was used the finite elements software Cast3M, wherethe described model is implemented [5]. The model is characterized by the parameters presented in Table 3.

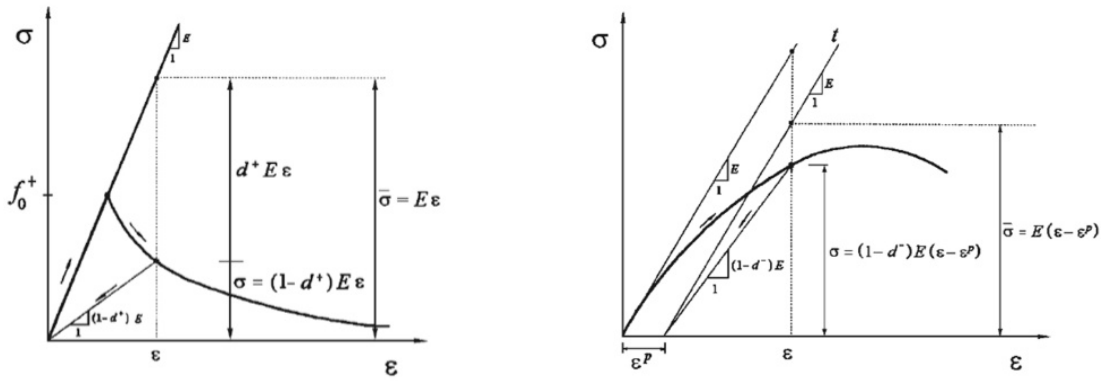

Fig. 1 Material behaviour [1]: Uniaxial tension (left). Uniaxial compression (right)

3. CALIBRATION BASED ON THE SIMPLE COMPRESSION CYCLIC TESTS

The material behaviour curves under compression were obtained through the simulation of a simple test on a 4-node finite element of unitary dimensions under monotonic and cyclic displacement laws. It was considered that the simulated specimen was composed of a homogeneous isotropic material characterized by the parameters given to the continuum damage model.

The calibration of the compressive branch of the material behaviour model was performed based on the results of the compression tests which were carried out for the walls B, D and F, [1]. The objective of this analysis was to fit the numerical 1D stress-strain response with the simple-compression experimental results through series of uni- and multi-parametric analyses. A different set of properties was used for each of the five wall typologies (1:1R, 1:1UR, 2:3R, 2:3UR, 1:1SL).

The majority of the parameters were taken from the experimental results. The Poisson ratios (v), the compressive peak stresses (f_u^-), the ultimate strains (ε_u^-), the elastic modulus (E) and the elastic limit stress (f_0^-) were obtained from the stress-strain diagrams. The density of the panel's material was obtained experimentally, (2200 kg/m^3 for the unreinforced three-leaf panels, 2500 kg/m^3 for the reinforced ones and 3200kg/m^3 for the single-leaf panels).

The adopted constitutive law uses two fitting points (P_1, P_2) which are located on the behaviour curve. Extensive sensitivity analysis was carried out considering different combinations of those points – P_1 (ε_1^-, σ_1^-) and P_2 (ε_2^-, σ_2^-) – until a good fit to the experimental results was achieved. For the equi-biaxial compressive ratio ($f_{0,2D}^-$) was adopted a value equal to 1. The characteristic length (l^*) of the used finite element in a 2D analysis is defined in (eq. 3):

$$l^* = \sqrt{\Delta A} \tag{3}$$

where: ΔA = the area associated to the integration point.

The calibrated continuum damage model was able to represent well the compression curves, in particular the first crack opening, the maximum strength and the deformation along the loading directions for both the monotonic and the cyclic tests. The parameters calibrated based on the monotonic compression test were used as a starting point for the model calibration based on the cyclic compression tests.

In what concerns the calibration based on the cyclic compression tests, the loading and re-loading behaviour had also to be simulated. As stone masonry is a very inhomogeneous material, it behaves with high plastic strains during the unloading and re-loading cycles. This behaviour is controlled, in the model, by the internal parameter β, which is used to calculate the residual plastic strains and, consequently, the cyclic un-loading and re-loading stiffness and energy dissipation in compression. Parameter $\beta$is calculated according to (eq. 4):

$$\beta = \frac{(E\varepsilon^{p-} - \sigma^{p-})f_u^-}{(E\varepsilon^{p-} - f_0^-)(\sigma^p + f_u^-)} \tag{4}$$

where:ε^{p-} and σ^{p-}= the reference strain and stress plastic parameters, E = the elastic modulus, f_u^- = the peak and elastic stress, f_0^-= the limit stress

This behaviour could not be accurately reproduced using the experimental values. To do so, unrealistic values would have to be adopted for the parameters that directly influence β, namely the plastic parameters (ε^{p-}) and (σ^{p-}), the elastic modulus (E) and the elastic limit stress (f_0^-). By assuming only experimental values it was chosen a reference point along the plastic branch of the curves so that the numerical un-loading and re-loading stiffness would be as close as possible to the experimental one.

Some results of the model calibration based on the monotonic and cyclic uni-axial compression tests law are shown in Fig. 2; the calibrated parameters for cyclic compression for all the wall typologies are presented in Table 1.

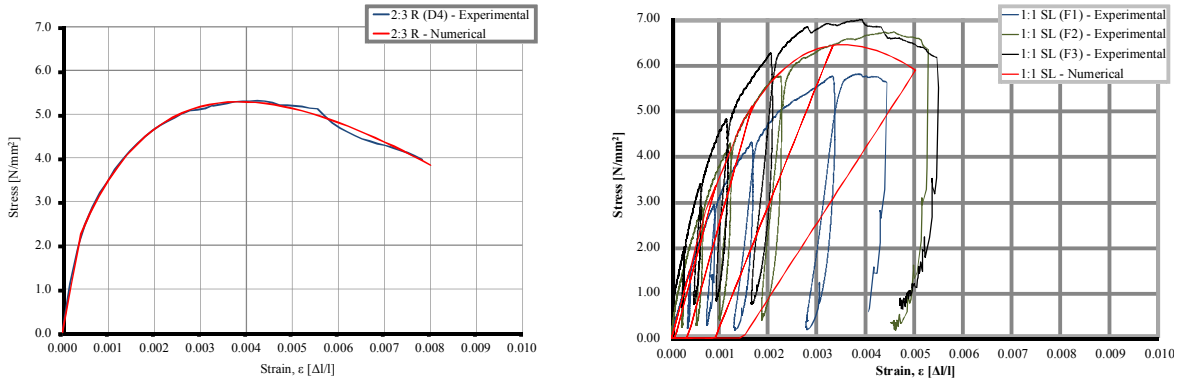

Fig. 2 Experimental and numerical curves for the cyclic compression tests. Monotonic compression test of reinforced wall in 2:3 (left). Cyclic compression test of single-leaf wall in 1:1 (right)

Table 1 Continuum damage model parameter values for the cyclic compression

		Parameters	*1:1 (UR)*	*1:1 (R)*	*2:3 (UR)*	*2:3 (R)*	*1:1 (SL)*
YOUN	E	Elastic modulus – 10 to 40% σ_{max} [N/m^2]	$3.0\cdot10^9$	$5.8\cdot10^9$	$2.2\cdot10^9$	$5.2\cdot10^9$	$3.9\cdot10^9$
NU	ν	Poisson ratio – 40% and 60% σ_{max} [-]	0.19	0.12	0.19	0.12	0.28
RHO	ρ	Density [kg/m^3]	2200	2500	2200	2500	3200
FC01	f_0^-	Elastic limit compressive stress [N/m^2]	$-0.92\cdot10^6$	$-2.04\cdot10^6$	$-1.46\cdot10^6$	$-2.0\cdot10^6$	$-2.74\cdot10^6$
RT45	$f_{0,2D}^-/f_{0,1D}^-$	Equi-biaxial compressive Ratio [-]	1	1	1	1	1
FCU1	f_u^-	Compressive peak stress [N/m^2]	$-2.6\cdot10^6$	$-4.30\cdot10^6$	$-2.21\cdot10^6$	$-4.64\cdot10^6$	$-6.5\cdot10^6$
EXTU	ε_u^-	Ultimate limit strain [-]	-0.005	-0.0057	-0.0043	-0.005	-0.005
EXTP	ε^{p-}	Reference strain for plastic parameter [-]	-0.0009	-0.0020	-0.0012	-0.0012	-0.0034
STRP	σ^{p-}	Reference stress for plastic parameter [-]	$-1.80\cdot10^6$	$-3.70\cdot10^6$	$-1.90\cdot10^6$	$-3.60\cdot10^6$	$-6.40\cdot10^6$
EXT1	ε_1^-	Fitting point 1 – Strain [-]	-0.0009	-0.0020	-0.0012	-0.0012	-0.0020
STR1	σ_1^-	Fitting point 1 – Stress [N/m^2]	$-1.80\cdot10^6$	$-3.7\cdot10^6$	$-1.90\cdot10^6$	$-3.6\cdot10^6$	$5.60\cdot10^6$
EXT2	ε_2^-	Fitting point 2 – Strain [-]	-0.005	-0.0052	-0.004	-0.005	-0.0044
STR2	σ_2^-	Fitting point 2 – Stress [N/m^2]	$-2.30\cdot10^6$	$-3.6\cdot10^6$	$-1.40\cdot10^6$	$-4.0\cdot10^6$	$-6.20\cdot10^6$

4. CALIBRATION BASED ON THE SHEAR-COMPRESSION TESTS

3.1. Model definition

The experimental shear-compression test results were simulated through a macro-modelling strategy, considering masonry as a homogeneous and isotropic material, using the non-linear continuum damage model previously described.

Fig. 3 Finite element model of the panels: mesh, boundary conditions and applied loads on the numerical simulation of the shear-compression tests. Numerical model (left). Experimental test of panel C8 (right)

For the calibration of the properties that define the compressive branch of the behaviour model it was used as starting point the properties that resulted from the previous calibration based on the cyclic simple-compression tests, (Table 1). In what concerns the definition of the tensile branch, the properties of the parameters were chosen in order to confer to the stone masonry a fragile low resistant behaviour, (Table 2). The tensile strength (f_t^+) for the different types of walls was takenfrom the shear-compression experimental tests. The tensile fracture energy (G_f) was adopted based on bibliographic research. According to thebibliography [6], for the tensile fracture energy a value between 10-100J is considered to be plausible and thus it was selected an average value of 50J. Moreover, an exponential softening behaviour (NCRI=1) with zero drop factor (Δf_0^+) was adopted to represent the tensile post peak behaviour.

Due to the significantly higher strength of the reinforced concrete beam, when compared to the masonry, and to the fact that the stresses will not exceed the elastic domain, the reinforced concrete

properties were defined as linear elastic and isotropic with E = 29 GPa, ν = 0.25 and ρ = 2500 kg/m^3. A plane stress state was assumed in all models, (Fig. 3), and the experimental boundary conditions and loading schemes were considered. Eight-node elements with a Gauss integration scheme (QUA8) were used.In the simulation of the shear-compression tests, the translational degrees of freedom (Ux, Uy) at the base of the model were constrained. The initial vertical pre-compression was applied to the nodes of the top surface of the reinforced concrete beam; the horizontal displacement laws were applied also on the beam, according to the real experimental procedure (Fig. 3).

Table 2 Continuum damage model parameter values – tensile branch

		Parameters	***1:1 (UR)***	***1:1 (R)***	***2:3 (UR)***	***2:3 (R)***	***1:1 (SL)***
GVAL	G_f	Tensile fracture energy [J]	50	50	50	50	50
FTUL	f_t^+	Tensile stress [N/m^2]	$0.05\cdot10^6$	$0.17\cdot10^6$	$0.06\cdot10^6$	$0.15\cdot10^6$	$0.17\cdot10^6$
REDC	Δf_0^+	Drop factor for peak tensile stress [-]	0	0	0	0	0
NCRI	–	Tensile softening criteria [-]	1	1	1	1	1

4.2. Calibration results

The application of the parameter values that resulted from the calibration based on the cyclic compression tests proven to be unsatisfactory when applied directly to the simulation of the shear compression tests. As so, further calibration of the model was required. The new calibration was done through a phenomenological fitting of the numerical curves to the experimental ones (horizontal force vs. measured displacement) through a series of uni- and multi-parametric analyses, paying particular attention to the structural elements stiffness, strength and ductility.Representative material the behaviour laws in tension and compression, (Fig. 4 and Fig. 5), capable of reproducing the in-plane behaviour under the different applied pre-compression levels, were defined for each type of tested panels. Thecalibrated parameters for each wall typology are shown in (Table 3).

Table 3 Parameter values from the calibration process based on the shear-compression tests

		Parameters	***1:1 (UR)***	***1:1 (R)***	***2:3 (UR)***	***2:3 (R)***
YOUN	E	Elastic modulus [N/m^2]	$3.3\cdot10^9$	$5.0\cdot10^9$	$3.0\cdot10^9$	$4.7\cdot10^9$
NU	ν	Poisson ratio [-]	0.19	0.12	0.19	0.12
RHO	ρ	Density [kg/m^3]	2200	2500	2200	2500
GVAL	G_f	Tensile fracture energy [J]	50	50	50	50
FTUL	f_t^+	Tensile stress [N/m^2]	$0.05\cdot10^6$	$0.17\cdot10^6$	$0.06\cdot10^6$	$0.15\cdot10^6$
REDC	Δf_0^+	Drop factor for peak tensile stress [-]	0	0	0	0
FC01	f_0^-	Elastic limit compressive stress [N/m^2]	$-0.85\cdot10^6$	$-1.5\cdot10^6$	$-0.5\cdot10^6$	$-1.5\cdot10^6$
RT45	$f_{0,2D}^-/ f_{0,1D}^-$	Equi-biaxial compressive Ratio [-]	1	1	1	1
FCU1	f_u^-	Compressive peak stress [N/m^2]	$-2.6\cdot10^6$	$-6.5\cdot10^6$	$-3.5\cdot10^6$	$-6.6\cdot10^6$
EXTU	ε_u^-	Ultimate limit strain [-]	-0.02	-0.025	-0.02	-0.025
EXTP	ε^{p-}	Reference strain for plastic parameter [-]	-0.0009	-0.0008	-0.00075	-0.0017
STRP	σ^{p-}	Reference stress for plastic parameter [-]	$-1.5\cdot10^6$	$-2.8\cdot10^6$	$-1.45\cdot10^6$	$-3.9\cdot10^6$
EXT1	ε_1^-	Fitting point 1 – Strain [-]	-0.0009	-0.0008	-0.00075	-0.0017
STR1	σ_1^-	Fitting point 1 – Stress[N/m^2]	$-1.5\cdot10^6$	$-2.8\cdot10^6$	$-1.45\cdot10^6$	$-3.9\cdot10^6$
EXT2	ε_2^-	Fitting point 2 - Strain [-]	-0.01	-0.016	-0.021	-0.023
STR2	σ_2^-	Fitting point 2 - Stress [N/m^2]	$-2.4\cdot10^6$	$-4.7\cdot10^6$	$-1.8\cdot10^6$	$-4.4\cdot10^6$
NCRI	–	Tensile softening criteria [-]	1	1	1	1

In (Table 4) it is presented the percentage variation of the behaviour model parameters in relation to the ones calibrated based on the cyclic compression tests. Although the calibrations were carried out in a rather limited number of tests in comparison to the universe of wall typologies and of properties inside the same typology, general principles, capable of characterizing the main trend of the behaviour

curves for the proper calibration of similar masonry typologies under different levels of pre-compression, were obtained.

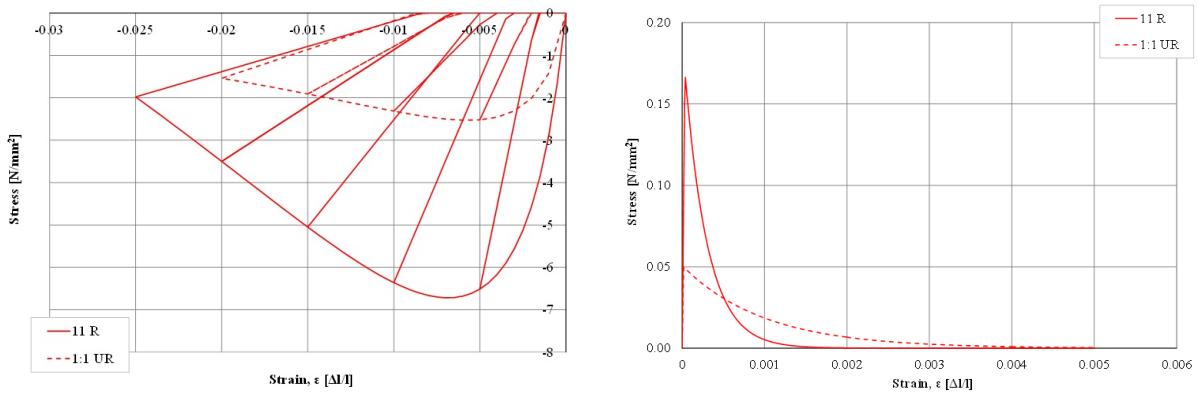

Fig. 4 Material behaviour laws for the wall panels in scale 1:1. Compressive behaviour (left). Tensile behaviour (right)

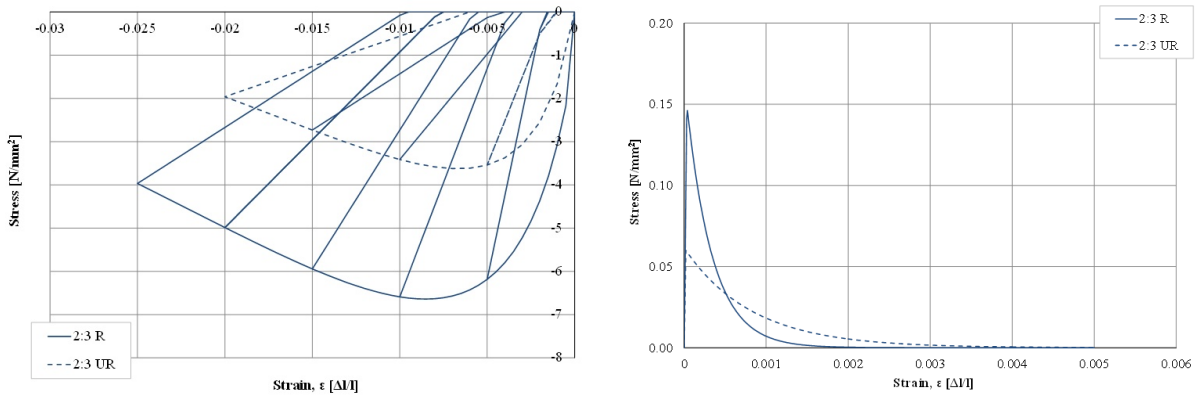

Fig. 5 Material behaviour laws for the wall panels in scale 2:3. Compressive behaviour (left). Tensile behaviour (right)

Table 4 Variation of the parameter values in relation to the calibration based on the cyclic compression tests

		Parameters	*1:1 (UR)*	*1:1 (R)*	*2:3 (UR)*	*2:3 (R)*
YOUN	E	Elastic modulus [%]	10	-14	36	-10
FC01	f_0^-	Elastic limit compressive stress [%]	-8	-26	-66	-25
FCU1	f_u^-	Compressive peak stress [%]	0	51	58	42
EXTU	ε_u^-	Ultimate limit strain [%]	300	339	388	400
EXTP	ε^{p-}	Reference strain for plastic parameter [%]	0	-60	-38	42
STRP	ε^{p-}	Reference stress for plastic parameter [%]	-17	-24	-24	8
EXT1	σ^{p-}	Fitting point 1 - Strain [%]	0	-60	-38	42
STR1	ε_1^-	Fitting point 1 - Stress [%]	-17	-24	-24	8
EXT2	σ_1^-	Fitting point 2 - Strain [%]	100	208	425	360
STR2	ε_2^-	Fitting point 2 - Stress [%]	4	31	29	10

The increase in the deformation and resistance capacity of the behaviour model, when compared with the calibration made based on the compression tests, is normal in the simulation of this type of tests where a highly plasticized localized area is solicited, for example, by the combined action of compression and flexion.

In Fig. 6 it is shown the numerically obtained response curves (envelope of the force vs. displacement diagram) for the panels in scale 1:1.

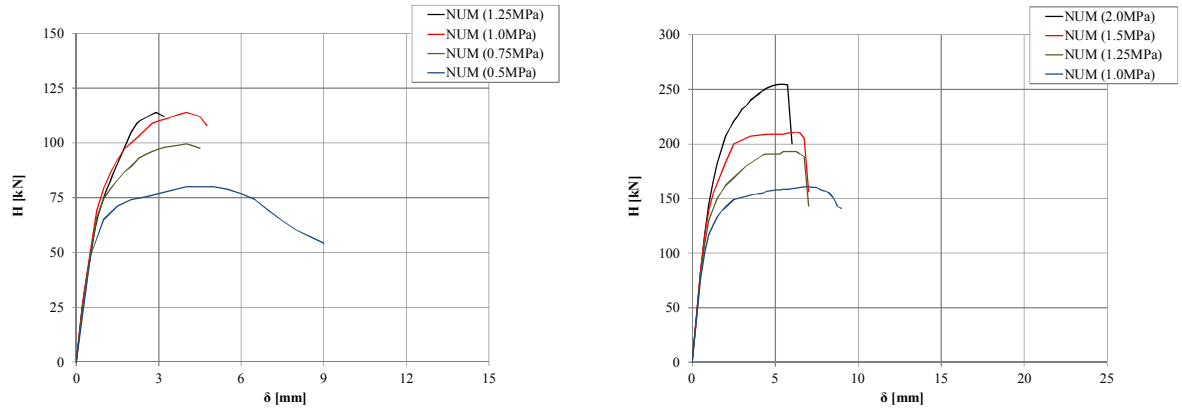

Fig. 6. Numerical (H vs. δ) response curve for the different panels in scale 1:1 and pre-compression levels. Unreinforced (left). Reinforced (right)

As it can be seenfrom the response curves comparison shown in Fig. 7 and the results in Table 5, in general a good and representative fit was achieved between the numerical and experimental.

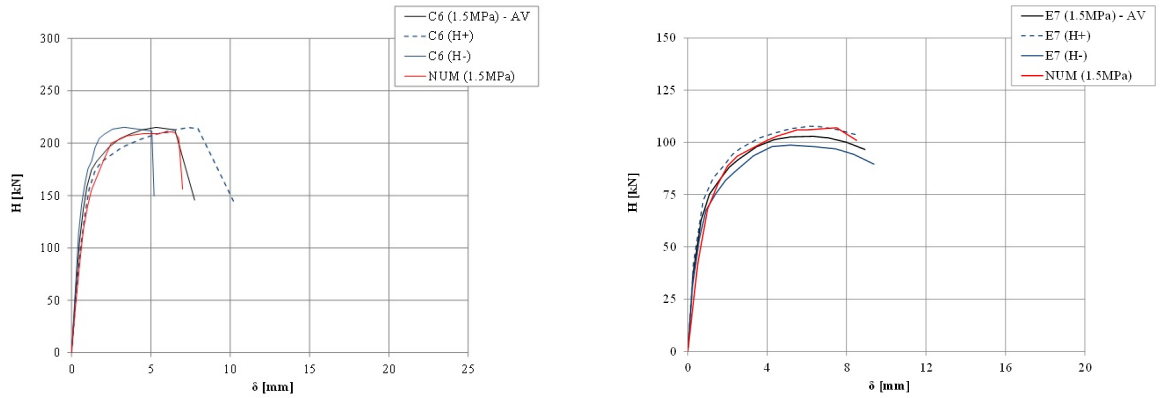

Fig. 7 Shear-compression envelope curves: experimental and numerical load displacement diagrams for the reinforced specimens. (a) $C6_{1:1}$ (1.5 MPa) and (b) $E7_{2:3}$ (1.5 MPa)

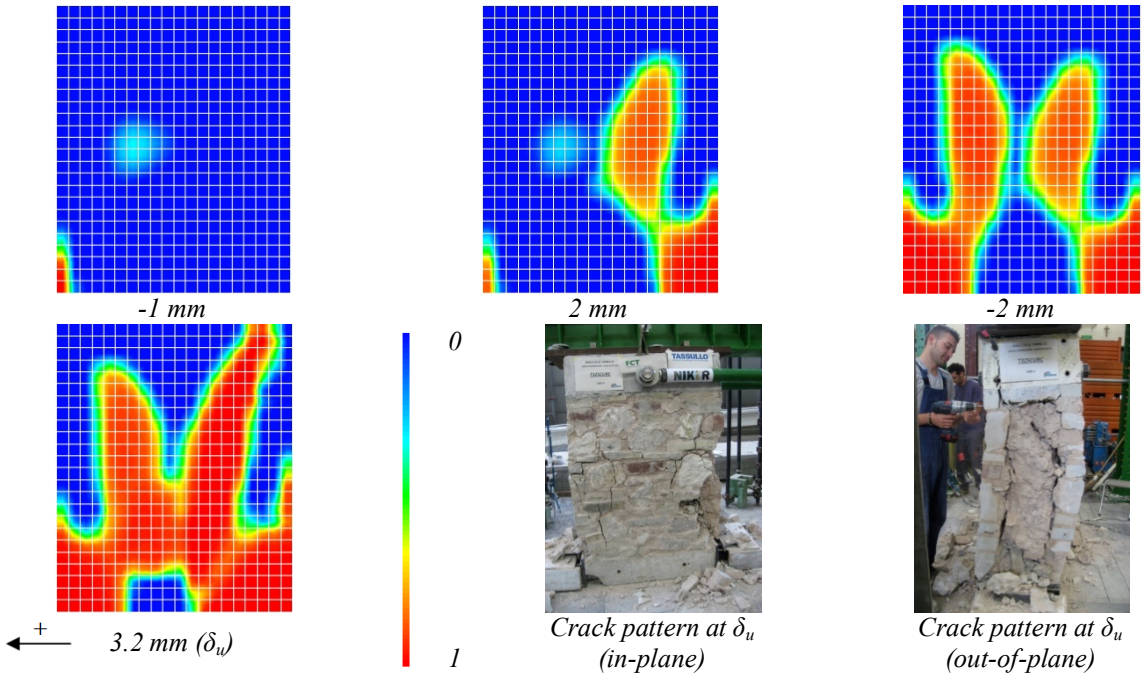

Fig. 8 Tensile damage (d^+) propagation in panel $C2_{1:1}$ (1.25MPa) and comparison with the real damage pattern at δ_u

The calibrated model was able to simulate well the initial elastic stiffness (K) and maximum horizontal loads (H_{max}). The resistance ratio $H_{max,n}/H_{max,e}$ presented in (Table 5) is approximately 1 for

all tested typologies of panels, in particular for the unreinforced ones. The reinforced panels (1:1 and 2:3) were in average slightly underestimated between 1 and 4%. In what concerns the displacement capacity, the behaviour model showed some limitations in capturing the displacement for maximum load (δ_{Hmax}) and the ultimate displacement (δ_u) in the reinforced specimens tested under the lowest pre-compression levels (1.0 MPa and 1.25 MPa) which had the behaviour governed by a rocking type mechanism. However, for the other reinforced specimens and for all the unreinforced ones the $\delta_{Hmax,n}/\delta_{Hmax,e}$ and $\delta_{u,n}/\delta_{u,e}$ ratios are approximately 1.
The behaviour model presented also important limitations in the simulation of the unload stiffness and of the energy dissipation, which are mainly due to the inability of this damage model to capture effects like the joints friction, phenomena related to the panels local behaviour.
The applied modelling strategy was able to reproduce the prevailing in-plane failure mechanisms and sequence of damage formation on the panels, with crack patterns similar with those observed experimentally, (Fig. 8). However, a 2D finite element analysis with shell elements is not capable of simulating the buckling of the external leaves developed, which is particularly presentin the unreinforced panels such as the case of panel $C2_{1:1}$.

Table 5 Comparison of the numerical and experimental maximum horizontal load (H_{max}), displacement for maximum load (δ_{Hmax}) and displacement at ultimate state (δ_u)

Specimens	*Experimental*			*Numerical*			$H_{max,n}/H_{max,e}$ [-]	$\delta_{Hmax,n}/\delta_{Hmax,e}$ [-]	$\delta_{u,n}/\delta_{u,e}$ [-]
	$H_{max,e}$ [kN]	$\delta_{Hmax,e}$ [mm]	$\delta_{u,e}$ [mm]	$H_{max,n}$ [kN]	$\delta_{Hmax,n}$ [mm]	$\delta_{u,n}$ [mm]			
C1 (1.0MPa)	116.3	4.0	6.7	114.0	4.0	5.0	0.98	1.0	0.75
C2 (1.25MPa)	104.6	2.4	2.8	114.0	2.9	3.2	1.1	1.2	1.1
C3 (0.75MPa)	77.0	2.5	4.3	99.6	4.0	4.5	1.3	1.6	1.1
C4 (0.5MPa)	76.0	6.4	10.3	80.0	5.0	9.0	1.1	0.78	0.87
Average							***1.1***	***1.15***	***0.96***
C5 (1.0MPa)	172.2	19.9	21.6	160.8	7.0	9.0	0.93	0.35	0.42
C6 (1.5MPa)	215.0	5.3	6.5	211.0	5.0	7.0	0.98	0.94	1.1
C7 (1.25MPa)	208.2	15.0	18.1	193.0	6.3	7.0	0.93	0.42	0.39
C8 (2.0MPa)	258.7	6.1	7.8	255.0	5.5	6.0	0.99	0.90	0.77
Average							***0.96***	***0.50***	***0.67***
E2 (1.0MPa)	67.6	5.1	6.7	67.8	5.0	5.4	1.0	0.98	0.81
E3 (0.75MPa)	53.4	4.9	6.8	56.8	5.5	6.5	1.1	1.1	0.96
E4 (1.25MPa)	73.3	3.6	6.2	75.3	4.5	4.9	1.0	1.3	0.79
Average							***1.0***	***1.1***	***0.85***
E5 (1.25MPa)	102.5	9.0	14.1	94.9	7.5	9.0	0.93	0.83	0.64
E6 (1.0MPa)	89.4	16.3	19.1	81.0	7.0	9.0	0.91	0.43	0.47
E7 (1.5MPa)	103.3	5.7	8.9	107	6.5	8.5	1.0	1.1	0.96
E8 (2.0MPa)	116.8	4.9	6.1	127	5.0	6.0	1.1	1.0	0.98
Average							***0.99***	***0.84***	***0.76***

5. CONCLUSIONS

The calibrated continuum damage behaviour model was able to represent well the compression curves, in particular the first crack opening, the ultimate load and deformability along the loading direction. However, the model didn't properly represent the cyclic un-loading and re-loading stiffness and, consequently, the energy dissipation in compression. In the simulation of the experimental shear-compression test results, the behaviour model allowed a good fit to the experimental results in terms of initial elastic stiffness and maximum horizontal loads for all specimens. In terms of displacement capacity, the behaviour model was not able to capture the displacement for maximum load (δ_{Hmax}) and the ultimate displacement (δ_u) of the reinforced specimens tested under the lowest pre-compression levels with behaviour governed by rocking mechanism. The applied modelling strategy was also able to reproduce the observed sequence of failure mechanisms and presented crack patterns consistent with the experimental ones. However, this type of modelling strategy is not capable of simulating the buckling of the external leaves developed, in particular, on the unreinforced panels.

ACKNOWLEDGEMENTS

The authors would like to thank FCT (Fundaçãopara a Ciência e a Tecnologia – The Foundation for Science and Technology) of Portugal and the NIKER project (New integrated knowledge based approaches to the protection of cultural heritage from Earthquake-induced risk) for the financial support provided for this research.

REFERENCES

[1] Silva B, Diagnosis and strengthening of historical masonry structures: numerical and experimental analyses. PhD Thesis, University of Padova, Italy, 2012.
[2] Faria R, Avaliação do comportamento sísmico de barragens de betão através de um modelo de dano contínuo. PhD Thesis, Faculty of Engineering, University of Porto, Portugal, 1994. (in Portuguese).
[3] CEA – Visual Cast3M – Guide d' utilisation. France, 1990.
[4] Faria R, Oliver J, Cervera M, A strain-based viscous-plastic-damage model for massive concrete structures. International journal of solids and structures 35(14): 1533-1558, 1998.
[5] Costa C, Implementation of the damage model in tension and compression with plasticity in Cast3m. Laboratório ELSA, JRC, Italy, 2004.
[6] Lourenço PB, Computational strategies for masonry structures. PhD Thesis. Delft University of Technology, Netherlands, 1996.